Available online at www.sciencedirect.com

SCIENCE DIRECT

ELSEVIER

Journal of Solid State Chemistry 177 (2004) 1501–1507

JOURNAL OF SOLID STATE CHEMISTRY

http://elsevier.com/locate/jssc

A new ferroelectric solid solution system of $LaCrO_3$–$BiCrO_3$

J.I.L. Chen, M. Mahesh Kumar, and Z.-G. Ye*

Department of Chemistry, Simon Fraser University, 8888 University Dr., Burnaby, BC, Canada V5A 1S6

Received 14 August 2003; received in revised form 3 November 2003; accepted 29 November 2003

Abstract

A new perovskite solid solution system of $(1-x)LaCrO_3$–$xBiCrO_3$ has been prepared by conventional solid-state reaction and sintering processes at 1200°C in a sealed Pt tube or a Bi_2O_3-rich environment. A clean orthorhombic phase of $LaCrO_3$-type structure is established at room temperature for compositions with $0 \leqslant x \leqslant 0.35$. The relative density, lattice parameters, sintering mechanism, microstructure and ferroelectricity of the compounds are investigated. The substitution of Bi_2O_3 for La_2O_3 is found to decrease the unit cell volume and increase the grain size of the ceramics. The relative density of the ceramics sintered at 1200°C is significantly improved from 40% for $LaCrO_3$ up to about 90% for $La_{0.65}Bi_{0.35}CrO_3$ through a liquid phase sintering mechanism. The ferroelectricity is revealed in $La_{1-x}Bi_xCrO_3$ with $0.1 \leqslant x \leqslant 0.35$ by dielectric hysteresis loops displayed at 77 K. The remnant polarization is found to increase with increasing Bi^{3+} content. The origin of the ferroelectricity is attributed to the structural distortion induced by the stereochemically active Bi^{3+} ion on the A site.

Keywords: Lanthanum bismuth chromite; Perovskite; Solid solutions; Solid-state synthesis; Ceramic sintering; Ferroelectricity; Solid-oxide fuel cells

1. Introduction

Lanthanum chromite, $LaCrO_3$, crystallizes in a distorted perovskite structure with an orthorhombic phase at room temperature. It belongs to the centrosymmetric space group *Pbnm* with a phase transition from the orthorhombic to rhombohedral phase observed at 260°C [1]. Unlike many perovskite-structured compounds that show ferroelectricity, no conclusive evidence of this trait has been found for $LaCrO_3$. Subba Rao et al. [2] studied the pyroelectric current and the electrical conductivity ($\log\sigma - 1/T$ relationship) of $LaCrO_3$, but did not find any peak or break which would otherwise suggest a ferroelectric–paraelectric transition. On the other hand, its high electronic conductivity, low ionic conductivity and good chemical stability in both oxidizing and reducing environments at high temperatures have made $LaCrO_3$ suitable for use as the interconnect material in solid-oxide fuel cells [3,4]. However, the challenge faced with the synthesis of $LaCrO_3$ is its poor sinterability and the resultant low density of $LaCrO_3$ ceramics due to its refractory nature and the volatilization of CrO_3 [5]. Several techniques were investigated to counter this problem, including (i) firing $LaCrO_3$ between Cr_2O_3 plates [6], (ii) substituting A or B site cations with alkaline earth or transition elements [7–12] and (iii) introducing a liquid phase through Ca or Co doping [13–15]. A large amount of work was reported on the cationic substitutions on the A or B sites, with the Ca or Sr-doped lanthanum chromites being the most optimal materials presently developed for fuel cell applications. The sintering temperature required to obtain dense ceramics, however, is still very high (about 1500°C). Therefore, one of the objectives of our present work is to improve the density of the $LaCrO_3$-type ceramics by partial substitution of Bi_2O_3 for La_2O_3 in $LaCrO_3$, which is expected to introduce a eutectic-like low melting in the La_2O_3–Cr_2O_3–Bi_2O_3 ternary system. The sintering temperature required to obtain dense $LaCrO_3$-type ceramics should therefore decrease.

Unlike its isostructural compound $BiFeO_3$, little is known about $BiCrO_3$, which is mainly because of the difficulties encountered in the synthesis of the pure phase. A pseudo-monoclinic structure at high temperature and a pseudo-triclinic phase below 127°C were reported earlier [16]. An orthorhombic perovskite structure with $a = 10.52$ Å, $b = 17.63$ Å and $c = 9.995$ Å

---

*Corresponding author. Fax: +1-604-291-3765.

E-mail address: zye@sfu.ca (Z.-G. Ye).

0022-4596/$ - see front matter © 2004 Elsevier Inc. All rights reserved.
doi:10.1016/j.jssc.2003.11.035

was suggested by Masuno [17]. In the work on the phase transitions in bismuth chromite, Reznitskii found that $BiCrO_3$ exhibits a polymorphic transition at 882°C and melts (and crystallizes) at 928°C [18]. A rapid increase of electrical conductivity of $BiCrO_3$ with temperature, from $8\times10^{-6}\,\Omega^{-1}\,cm^{-1}$ at 350°C to $3\times10^{-1}\,\Omega^{-1}\,cm^{-1}$ in the liquid phase, was observed. These results, however, have not been confirmed. On the other hand, recent theoretical calculations by Hill et al. [19] suggested a Bi-induced distortion in the structure that could be antiferroelectric and/or antiferrodistortive. They also predicted antiferromagnetism in $BiCrO_3$. The stereochemical activity of the lone pair electrons on Bi^{3+} leads us to suspect some ferroelectricity in this system. If this were true, then the origin of ferroelectricity would be a relative Bi–O displacement in the structure rather than the B-site distortion found in conventional perovskite ferroelectrics. Since pure $BiCrO_3$ is hard to prepare, its solid solution with other compounds may provide an indirect method for studying its structural chemistry and physical properties.

This paper reports the results obtained on the synthesis, crystal structure, sintering, microstructure and ferroelectricity of a new solid solution system between $LaCrO_3$ and $BiCrO_3$.

2. Experimental

Compounds of $(1-x)LaCrO_3$–$xBiCrO_3$ (with nominal compositions of $x = 0$, 0.1, 0.2, 0.3, 0.35 and 0.4) were prepared by conventional solid-state reactions using stoichiometric amounts of the starting oxides, La_2O_3 (99.9%), Cr_2O_3 (99.7%) and Bi_2O_3 (99.95%). The mixtures were thoroughly ground for 2 h and pressed into pellets of 1 cm in diameter. With the exception of $LaCrO_3$ which was synthesized in air, the pellets of the mixtures were fired either in a sealed Pt tube or a Bi_2O_3-rich environment. For the synthesis in Pt tube, the pellets were carefully broken up into smaller pieces and placed inside a Pt tube (I.D. = 6 mm, O.D. = 8 mm) which was then sealed and heated. For the synthesis in a Bi_2O_3-rich environment, 1 wt% of polyvinyl alcohol was added as the binding agent during grinding. The pellets were first preheated at 700°C in air for 1 h to remove the binder. They were then fired and sintered in a closed Bi_2O_3-rich environment which was aimed to reduce the volatilization of bismuth oxide. The closed Bi_2O_3-rich environment was created in an alumina crucible filled with 5–10 g of Bi_2O_3 powder. The pellets were put on a Pt plate suspended above the Bi_2O_3 powder in the crucible, which was sealed to an alumina lid with alumina cement. For both synthetic processes, the pellets were heated and sintered at 1200°C for 5–8 h in order to obtain the pure solid solution of $LaCrO_3$-type phase.

The crystal structural characterization of $LaCrO_3$ and the solid solutions were performed at room temperature using a Phillips powder X-ray diffractometer with Cu$K\alpha$ radiation in the range of $20\leqslant 2\theta\leqslant 80°$, at an increment of 0.02° and an exposure time of 2 s/step. LaB_6 was used as an internal reference and the lattice parameters were refined using XLAT program.

The density of the ceramics was measured using the Archimedes method in water. Differential thermal analysis (DTA) was performed using Seiko Instrument TG/DTA 6300 with α-alumina as the reference in order to study the sintering mechanism. A sample of 20 mg was loaded in a Pt pan and heated at a rate of 5°C/min up to 1050°C and cooled down at the same rate. The microstructure and grain morphology of the ceramics were examined by scanning electron microscopy using Bausch & Lomb 2100 Nanolab (B&L) or FEI Dual-Beam Strata 235 (FEI 235) microscope. Dielectric hysteresis loops were displayed at 77 K (in liquid N_2) with an RT66A Testing System based on a Sawyer–Tower circuit, at a frequency of 5 Hz with various sense capacitors ranging from 0.33 to 0.78 μF.

3. Results and discussion

3.1. Formation of solid solutions

Synthesis of the $La_{1-x}Bi_xCrO_3$ solid solutions is first carried out in a closed Bi_2O_3-rich environment to reduce the volatilization of bismuth oxide from the ceramics. This method is, however, only effective in the temperature range of 1100–1250°C. At temperatures below 1100°C, not enough bismuth oxide vapor pressure from the Bi_2O_3 powder is created inside the sealed chamber, while at temperatures above 1250°C, even a high bismuth oxide pressure cannot prevent the volatilization of bismuth oxide from the sample. The loss of bismuth oxide is monitored by measuring the weight change of the pellets before and after sintering. It varies from 0.5% to 3% for the solid solutions prepared by this process. In the sintering process in the Bi_2O_3-rich environment, the condensation of bismuth oxide vapor as the temperature cools down could lead to the deposition of Bi_2O_3 on the surface of the pellets, which might diffuse into the pellets and affect the composition of the ceramics. In order to achieve a better stoichiometry for the composition of the solid solutions, synthetic process in a sealed Pt tube is carried out separately and the results from both methods are compared. Pt tube provides a closed inert environment and thereby effectively reduces the volatilization of bismuth oxide to almost null, as proved by zero weight loss. Therefore, the composition of the samples sintered in Pt tube is “as prepared”. Comparison of the structural parameters and physical properties of the samples prepared by the two methods shows no significant difference between them (see below). We can thereby confirm that the compositions of the solid solutions prepared in Bi_2O_3-rich environment are very close to the nominal composition.

As the Bi^{3+} content increases in the solid solution system, the synthesis time or temperature for obtaining the pure $LaCrO_3$-type phase also increases in both processes; at 1200°C, a soaking time of 5 h is enough for compositions with $0 \leqslant x \leqslant 0.2$, while 7–8 h is necessary for compositions with $x \geqslant 0.3$. With increasing Bi^{3+} content, the pellets of $La_{1-x}Bi_xCrO_3$ solid solutions darken from the green color of $LaCrO_3$, which results from the dark black color of $BiCrO_3$ as observed in our initial synthesis of $BiCrO_3$ in an inert atmosphere.

The X-ray diffraction spectra of the $La_{1-x}Bi_xCrO_3$ solid solutions with $0 \leqslant x \leqslant 0.35$ all show a clean orthorhombic phase of $LaCrO_3$-type at room temperature, as shown in Fig. 1. The lattice parameters of pure $LaCrO_3$ are refined to be $a = 5.5032 \pm 0.0011$ Å, $b = 5.4938 \pm 0.002$ Å, and $c = 7.7562 \pm 0.0021$ Å, in close agreement with previously reported data [8,15]. This confirms the structural feature of $LaCrO_3$ with a being slightly greater than b, in contrast to the majority of orthorhombic perovskites of *Pbnm* type. The calculations on lattice parameters have shown a decrease in a with increasing Bi^{3+} content in $La_{1-x}Bi_xCrO_3$. It is known that the octahedral tilting in the orthorhombic perovskite of this type usually causes a contraction in a [20]. Thus, it seems that the substitution of Bi^{3+} for La^{3+} in the solid solutions enhances the tilting of octahedrons. Fig. 2 shows that the calculated unit cell volume of $La_{1-x}Bi_xCrO_3$ increases slightly from $LaCrO_3$ at low substitution and then decreases at higher substitution (for $x > 0.10$). The shrinkage of the unit cell volume is mainly attributed to the Bi–O distortion in the structure (see discussion in Section 3.4) as the ionic radii of La^{3+} and Bi^{3+} in coordination VIII (1.30 and 1.31 Å, respectively [21]) are very similar. A detailed analysis of the crystal structure of $La_{1-x}Bi_xCrO_3$ is underway to illustrate the effect of Bi^{3+} on the lattice parameters and octahedral tilting in this solid solution system, the results of which will be published elsewhere.

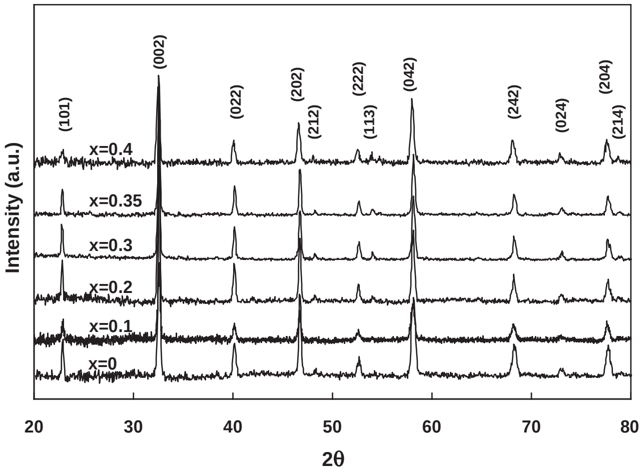

Fig. 1. XRD patterns as a function of composition for the $(1-x)LaCrO_3$–$xBiCrO_3$ solid solution system sintered in a Bi_2O_3-rich environment at 1200°C.

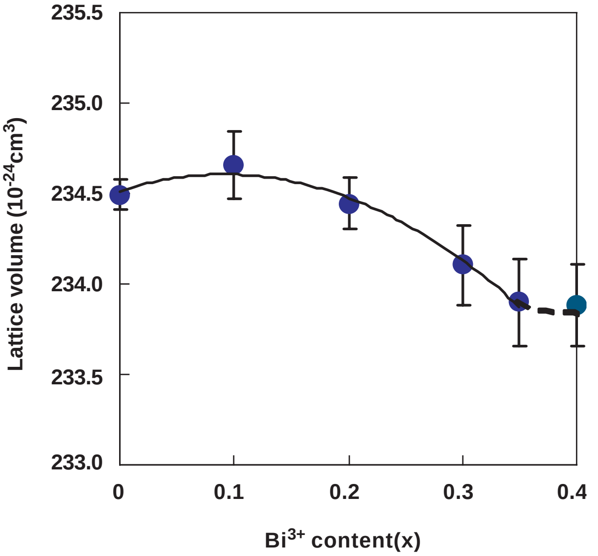

Fig. 2. Variations of unit cell volume as a function of composition for the $(1-x)LaCrO_3$–$xBiCrO_3$ solid solution system prepared in a Bi_2O_3-rich environment.

$La_{0.6}Bi_{0.4}CrO_3$ was also synthesized in Bi_2O_3-rich environment at 1250°C. Although the X-ray spectrum shows a clean orthorhombic phase (Fig. 1), its unit cell volume exhibits the same value as $La_{0.65}Bi_{0.35}CrO_3$, indicating that the limit of the solubility for the substitution of Bi^{3+} for La^{3+} has been reached at $x = 0.35$. Thus, pure solid solutions of $LaCrO_3$-type phase are formed in the $(1-x)LaCrO_3$–$xBiCrO_3$ system for the composition range of $0 \leqslant x \leqslant 0.35$. For compositions with greater than 35 mol% of $BiCrO_3$, the volatilization of bismuth oxide becomes too severe to form a pure phase above 1200°C, thus hindering the formation of the solid solution for the entire series of the system. The X-ray spectra in Fig. 1 also show the growth of several peaks (2 1 2, 1 1 3, and 2 1 4) as Bi^{3+} content is increased. Since bismuth has more electrons than lanthanum and thereby a higher scattering power, the intensity of certain Bragg peaks is expected to increase.

3.2. *Sintering of ceramics*

With the substitution of $BiCrO_3$ for $LaCrO_3$, the density of the ceramics increases from 3 g/cm^3 (of $LaCrO_3$) to 6.5 g/cm^3 at the limit of the solid solution system ($x = 0.35$) when sintered at 1200°C. The relative density (i.e., percentage of the theoretical density) is drastically improved from 40% for $LaCrO_3$ up to about 90% for $x = 0.35$. The two sintering processes yield similar results. Fig. 3 shows the variation of the relative density of the $La_{1-x}Bi_xCrO_3$ ceramics sintered in a Bi_2O_3-rich environment as a function of Bi^{3+} content. Note that typical Sr-modified lanthanum chromite ceramics ($La_{0.7}Sr_{0.3}CrO_3$) so far prepared by conventional solid-state reaction required sintering at 1500°C to obtain a relative density of about 90% [12]. The same density has been achieved in this work on $La_{1-x}Bi_xCrO_3$ ceramics with $0.3 \leqslant x \leqslant 0.35$ at a sintering temperature 300°C lower than what was required for $La_{0.7}Sr_{0.3}CrO_3$. This is a significant improvement in the sinterability of the $LaCrO_3$-type ceramics that are potentially useful in many applications.

The sintering mechanism of the $La_{1-x}Bi_xCrO_3$ ceramics is deduced from the DTA. Fig. 4 shows the DTA curves for the mixture of starting metal oxides ($0.65La_2O_3 + 0.35Bi_2O_3 + Cr_2O_3$) and for the solid solution of $La_{0.65}Bi_{0.35}CrO_3$ synthesized in Pt tube. For the starting metal oxide mixture, an endothermic event at 955°C during heating and an exothermic event at 933°C during cooling are observed (Fig. 4a and b). On the other hand, the DTA curve for the $La_{0.65}Bi_{0.35}CrO_3$ solid solution does not show any peak (Fig. 4c). The endothermic peak in the starting oxide mixture can be attributed to a eutectic-like partial melting event that occurs in the ternary system of La_2O_3–Cr_2O_3–Bi_2O_3 due to the presence of the low-melting-point Bi_2O_3 (m.p. = 825°C). The partial melting of the system gives rise to a liquid phase at the grain boundary, which favors the sintering of dense ceramics at a relatively low temperature.

Since the pure solid solution cannot be formed completely at 1050°C upon the DTA heating run in open air, the solidification of the liquid phase takes place upon cooling of the oxide mixture, as revealed by the exothermic peak (Fig. 4b). The solidification occurs at a lower temperature (933°C) than the melting (955°C), indicating a supercooling phenomenon. Moreover, upon cooling, the system may contain the solid solution of $La_{1-y}Bi_yCrO_3$ partially formed during the heating process in addition to the remaining oxides. $La_{1-y}Bi_yCrO_3$ is expected to have a lower melting point than the refractory La_2O_3 (m.p. = 2300°C) due to the incorporation of Bi_2O_3. Such a pseudo-quaternary system should exhibit a eutectic-like melting point lower than that of the initial ternary system. Therefore, the solidification is observed at an even lower temperature with a significant thermal hysteresis.

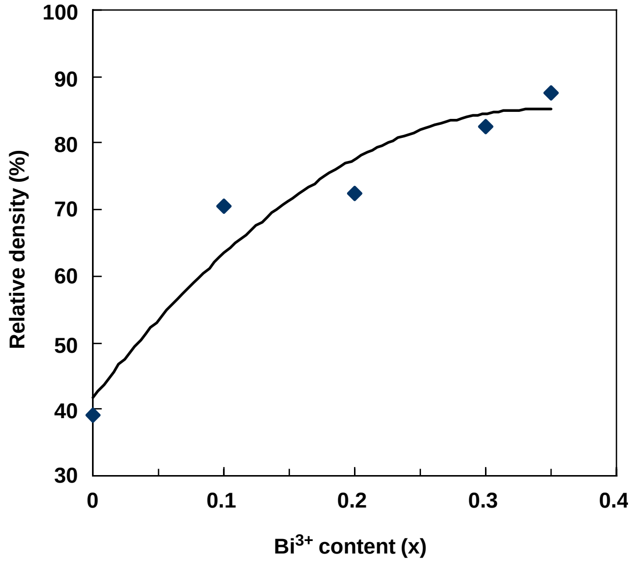

Fig. 3. Relative density as a function of x for $(1-x)LaCrO_3$–$xBiCrO_3$ ceramics sintered in a Bi_2O_3-rich environment at 1200°C.

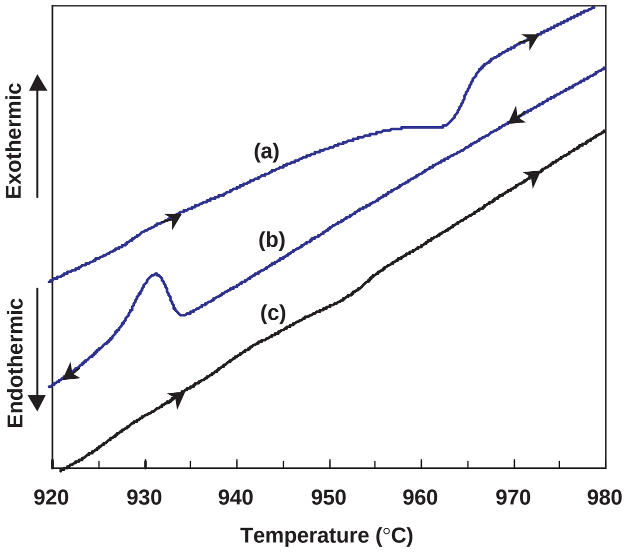

Fig. 4. DTA curves (at 5°C/min) for the starting metal oxide mixture of ($0.65La_2O_3 + 0.35Bi_2O_3 + Cr_2O_3$) (a and b) and for the solid solution of $La_{0.65}Bi_{0.35}CrO_3$ synthesized in a Pt tube (c).

The transient liquid phase has disappeared in the solid solution as Bi^{3+} becomes fully incorporated into the $LaCrO_3$-type structure at higher temperatures. As a result, no melting behavior is detected by DTA for $La_{0.65}Bi_{0.35}CrO_3$ upon heating. This confirms the presence of the liquid phase upon the heating of the metal oxide mixture and attests to the sintering mechanism of the $La_{1-x}Bi_xCrO_3$ ceramics deduced above.

Fig. 5 shows the DTA curves for the mixture of ($Bi_2O_3 + Cr_2O_3$). An endothermic event is observed at 931°C and an exothermic event at 924°C. These temperatures agree with those previously reported for the melting and solidification of $BiCrO_3$ [18]. However, since no pure $BiCrO_3$ phase can be formed after heating at 1000°C, it is expected that the melting and solidification events detected in our DTA experiments are related to a eutectic-like behavior of the Bi_2O_3–Cr_2O_3 system with the presence of partially formed $BiCrO_3$. Note that the melting temperature for the metal oxide mixture containing La_2O_3, Bi_2O_3 and Cr_2O_3 is higher than that for the mixture containing only Bi_2O_3 and Cr_2O_3, as can

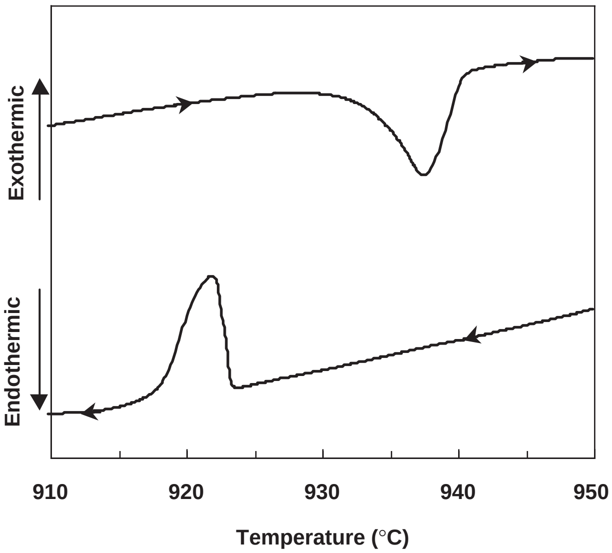

Fig. 5. DTA curves (at 5°C/min) for the starting metal oxide mixture of ($Bi_2O_3 + Cr_2O_3$).

be expected from the presence of the refractory La_2O_3 in the former system. This also confirms that the liquid phase formed during the sintering of $La_{1-x}Bi_xCrO_3$ ceramics is a result of the eutectic-like melting in the ternary system of La_2O_3–Cr_2O_3–Bi_2O_3, but not the direct melting of "$BiCrO_3$".

3.3. Microstructures

Fig. 6 shows the SEM micrographs of the surfaces of $La_{1-x}Bi_xCrO_3$ ceramics sintered at 1200°C for 5–8 h. No significant difference was observed for the same composition sintered in the two different processes. The grain size grows with increasing Bi_2O_3 content, from an average of less than 1 μm in $LaCrO_3$ and $La_{0.9}Bi_{0.1}CrO_3$ to greater than 2 μm in $La_{0.7}Bi_{0.3}CrO_3$. In Figs. 6b and c, the particles on the surface of $La_{0.8}Bi_{0.2}CrO_3$ and $La_{0.7}Bi_{0.3}CrO_3$ ceramics are densely packed with very few pores. The grain growth and densification can be attributed to the increasing amount of transient liquid phase at grain boundary, which brings the grains closer in contact with each other, as Bi^{3+} substitution increases. Earlier study by Chakraborty and Maiti [22] showed that Bi_2O_3 is a very effective sintering aid for $La(Sr)MnO_3$. They found that Bi^{3+} goes into the La^{3+} site to form a complete solid solution and enhances the sintering process by increasing the overall diffusion rate of the A-site ions. In the $La_{1-x}Bi_xCrO_3$ system, not only does Bi_2O_3 form a solid solution with $LaCrO_3$, but it also introduces a transient liquid phase during sintering that enhances the grain growth and densification of the ceramics.

The SEM micrographs of the $La_{0.65}Bi_{0.35}CrO_3$ ceramics (not shown) also reveal partial melting at the grain boundary when sintered at 1200°C, which is justifiable

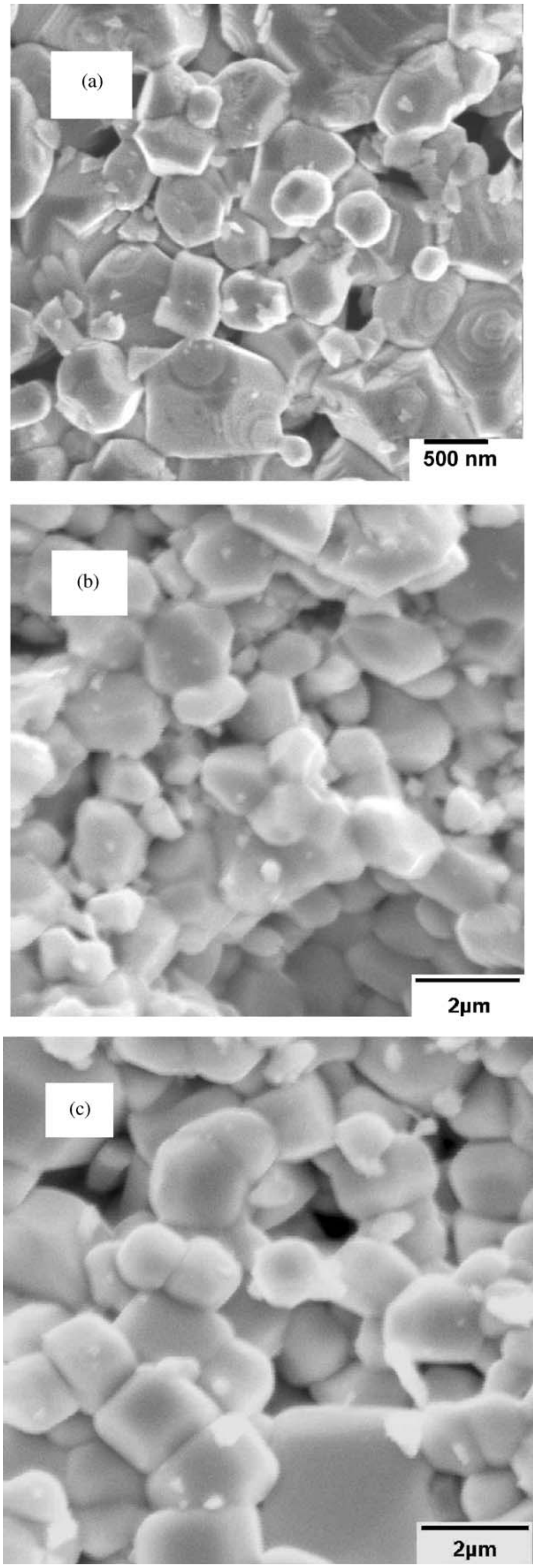

Fig. 6. SEM micrographs of the surface of $(1-x)LaCrO_3$–$xBiCrO_3$ ceramics sintered in a Pt tube with (a) $x = 0.1$ (taken with FEI 235), (b) $x = 0.2$ (B&L) and (c) $x = 0.3$ (B&L).

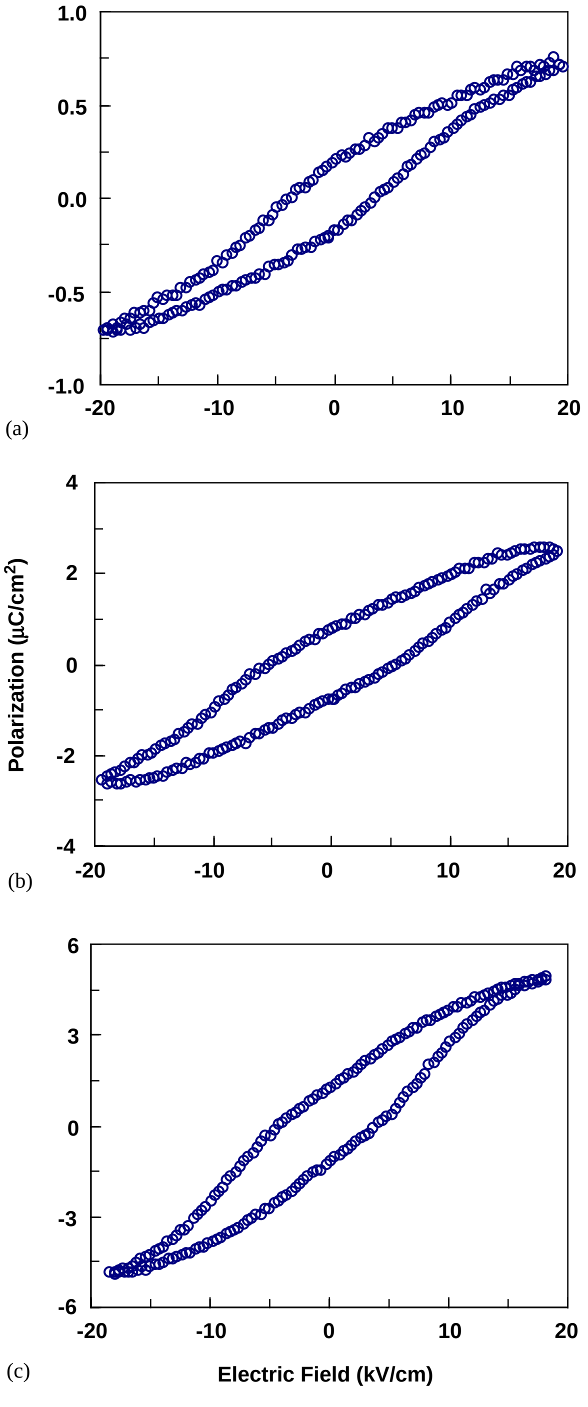

Fig. 7. Dielectric hysteresis loops displayed at 77 K for $(1-x)\mathrm{LaCrO_3}$–$x\mathrm{BiCrO_3}$ ceramics sintered in a Pt tube (in Sawyer–Tower mode): (a) $x=0.2$ ($C_{\mathrm{sense}}=0.33\,\mu\mathrm{F}$), (b) $x=0.3$ ($C_{\mathrm{sense}}=0.50\,\mu\mathrm{F}$), and (c) $x=0.35$ ($C_{\mathrm{sense}}=0.78\,\mu\mathrm{F}$).

as the melting temperature of the $\mathrm{La_{1-x}Bi_xCrO_3}$ solid solutions should decrease with increasing $\mathrm{Bi_2O_3}$ content.

3.4. Ferroelectricity

In search for ferroelectricity in the solid solutions of $\mathrm{La_{1-x}Bi_xCrO_3}$, the polarization versus bipolar electric field strength is measured for $0\leqslant x\leqslant 0.35$. The dielectric hysteresis loops for compositions are displayed at 77 K for compositions with $0.1\leqslant x\leqslant 0.35$ by a Sawyer–Tower circuit using various sense capacitors (Fig. 7), indicating the ferroelectric behavior for the solid solutions. With increasing $\mathrm{Bi^{3+}}$ content, the remnant polarization increases rapidly (Table 1) and the hysteretic behavior becomes more apparent. The increase of remnant polarization with increasing $\mathrm{Bi^{3+}}$ substitution suggests that the spontaneous polarization originates from the $\mathrm{Bi^{3+}}$ ions introduced in the solid solutions. Due to the high conductivity of the ceramics, no hysteresis loops could be obtained at room temperature. $\mathrm{LaCrO_3}$ does not show any hysteretic behavior even at 77 K, confirming that it is not a ferroelectric material.

Table 1
Variation of remnant polarization (P_{r}) as a function of composition for $(1-x)\mathrm{LaCrO_3}$–$x\mathrm{BiCrO_3}$ ceramics measured at 77 K by dielectric hysteresis loops

x	0.1	0.2	0.3	0.35
P_{r} ($\mu\mathrm{C/cm^2}$)	0.029	0.190	0.748	1.269

The ferroelectricity in the solid solutions may have originated from the distortion of Bi–O coordination environment as a result of the stereochemical activity of $\mathrm{Bi^{3+}}$ ion. Neither $\mathrm{Cr^{3+}}$ nor $\mathrm{La^{3+}}$ is displaced from their centrosymmetric position in $\mathrm{LaCrO_3}$. In contrast, it has been shown that the $(6s)^2$ electrons of $\mathrm{Bi^{3+}}$ can hybridize with its $6p$ orbitals and subsequently mix with $2p$ of oxygen to form a space-filling localized lobe, which in turn pushes away its neighboring atoms causing a structural distortion [19]. Therefore, the spontaneous polarization is more likely due to the structural distortion induced by $\mathrm{Bi^{3+}}$ on the A site rather than by any displacement of $\mathrm{Cr^{3+}}$ on the B site as commonly observed in conventional ferroelectric perovskites.

4. Conclusions

New solid solutions of $(1-x)\mathrm{LaCrO_3}$–$x\mathrm{BiCrO_3}$ ($0\leqslant x\leqslant 0.35$) have successfully been synthesized at 1200°C by solid-state reactions in a $\mathrm{Bi_2O_3}$-rich environment and a sealed Pt tube. The solid solution compounds crystallize in a $\mathrm{LaCrO_3}$-type orthorhombic perovskite phase with the lattice volume decreasing as Bi content is increased. The substitution of $\mathrm{Bi_2O_3}$ for $\mathrm{La_2O_3}$ significantly increases the grain size and density of the $\mathrm{LaCrO_3}$-type ceramics (up to 90%) by introducing a eutectic-like low melting in the system of $\mathrm{La_2O_3}$–$\mathrm{Cr_2O_3}$–$\mathrm{Bi_2O_3}$. The mechanism of the ceramic sintering is related to a transient liquid phase present in the ceramics prior to the complete formation of the solid solutions. The ferroelectricity has been revealed for the first time in these solid solution compounds by dielectric hysteresis loops displayed at 77 K. The spontaneous polarization increases with increasing Bi^{3+} content. The ferroelectricity in $La_{1-x}Bi_xCrO_3$ is believed to have originated from the structural distortion induced by the stereochemically active lone pair electrons of Bi^{3+} ion on the A site of the perovskite structure.

The significant improvement in the sinterability and densification of the $LaCrO_3$-type ceramics by the substitution of Bi_2O_3 points to a new route to the sintering of highly densified interconnect materials for solid-oxide fuel cells. In practical applications, however, one should be aware of the susceptibility of Bi^{3+} to form metallic Bi in reducing atmospheres at high temperatures. Since the density of the ceramics is dramatically increased by a relatively low Bi^{3+} substitution rate, a balance between the sinterability (density) and the chemical stability of the ceramics can be achieved and optimized in order to offset this drawback. On the other hand, the ferroelectricity discovered in $La_{1-x}Bi_xCrO_3$ entitles these compounds as a new class of ferroelectric materials formed by the peculiar crystal chemistry of Bi^{3+} ion. Further investigation of the detailed crystal structure is underway to illustrate the molecular mechanism underlying the ferroelectricity in the $La_{1-x}Bi_xCrO_3$ solid solutions.

Acknowledgments

The authors would like to thank W. Chen for technical help and Y. Bing for helpful discussion. This work was supported by the Natural Science and Engineering Research Council of Canada (NSERC).

References

[1] S. Geller, Acta Crystallogr. A 10 (1957) 243–248.
[2] G.V. Subba Rao, G.V. Chandrashekhar, C.N.R. Rao, Solid State Commun. 6 (1968) 177–179.
[3] W. Baukal, W. Kuhn, H. Kleinschmager, F.J. Rohr, J. Power Sources 1 (1976–1977) 203–213.
[4] W. Feduska, A.O. Isenberg, J. Power Sources 10 (1983) 89–102.
[5] D.B. Meadowcroft, J.M. Wimmer, Am. Ceram. Soc. Bull. 58 (1979) 610–615.
[6] L.-W. Tai, P.A. Lessing, J. Am. Ceram. Soc. 74 (1991) 155–160.
[7] P.S. Devi, M.S. Rao, Mater. Res. Bull. 28 (1993) 1075–1082.
[8] C.P. Khattak, D.E. Cox, Mater. Res. Bull. 12 (1977) 463–471.
[9] S. Hayashi, K. Fukaya, H. Saito, J. Mater. Sci. Lett. 7 (1988) 457–458.
[10] F. Jin, T. Endo, H. Takizawa, M. Shimada, J. Solid State Chem. 113 (1994) 138–144.
[11] T.R. Armstrong, J.S. Hardy, S.P. Simner, J.W. Stevenson, in: S.C. Singhal, M. Dokiya (Eds.), Proceedings of the Sixth International Symposium on Solid Oxide Fuel Cells, Vol. 99-19, Electrochemical Society, Pennington, NJ, 1999, pp. 706–715.
[12] S. Simner, J. Hardy, J. Stevenson, T. Armstrong, J. Mater. Sci. 34 (1999) 5721–5732.
[13] L.A. Chick, J. Liu, J.W. Stevenson, T.R. Armstrong, D.E. McCready, G.D. Maupin, G.W. Coffey, C.A. Coyle, J. Am. Ceram. Soc. 80 (1997) 2109–2120.
[14] R. Koc, H.U. Anderson, J. Eur. Ceram. Soc. 15 (1995) 867–874.
[15] M. Mori, N.M. Sammes, Solid State Ionics 146 (2002) 301–312.
[16] F. Sugawara, S. Ida, Y. Syono, S. Akimoto, J. Phys. Soc. Japan 25 (1968) 1553–1558.
[17] K. Masuno, J. Chem. Soc. Japan 90 (1969) 1122–1127.
[18] L.A. Reznitskii, Izv. Akad. Nauk SSSR Neorg. Mater. 10 (1974) 1156 (Inorg. Mater. (USSR) (1974) 993–994).
[19] N.A. Hill, P. Bättig, C. Daul, J. Phys. Chem. B 106 (2002) 3383–3388.
[20] R.H. Mitchell, Perovskites: Modern and Ancient, Almaz Press, Thunder Bay, 2002.
[21] R.D. Shannon, Acta Crystallogr. A 32 (1976) 751–767.
[22] A. Chakraborty, H.S. Maiti, Ceram. Int. 25 (1999) 115–123.